

Supplementary information for

Anion-order driven polar interfaces at LaTiO₂N surfaces

by

Silviya Ninova and Ulrich Aschauer

S1 Surfaces

We work with asymmetric slabs to describe the LaTiO₂N surfaces for the convenience of having stoichiometric and electroneutral simulation cells. The differently charged surface terminations, however, give rise to an artificial electric field across the vacuum and in the material. The former is corrected by a dipole corrections that adds an opposite electric field over a distance of 0.25 Å in the center of the vacuum region. The remaining electric field inside the material is generally weaker, as a result of screening. To determine if it affects the geometry in a significant way, we determine the internal electric field from a linear fit of the macroscopic average inside unrelaxed asymmetric slab and compare it to the symmetric one that is generally assumed to be a better choice to cancel this field.¹ We find that for model B the field inside the asymmetric slab is 0.12 eV/Å, whereas in the symmetric slab we find fields of 0.07 eV/Å and 0.02 eV/Å in the top and bottom half of the slab, the difference in the two half-slabs arising from the slight non-orthorhombicity of the cell that also manifests in the small potential step in the vacuum (Figure S1). The fields in symmetric and asymmetric slabs are thus of similar magnitude and we expect them to affect the geometry to a similar extent. Moreover a symmetric slab would not entirely cancel the internal electric field due to differently charged planes.

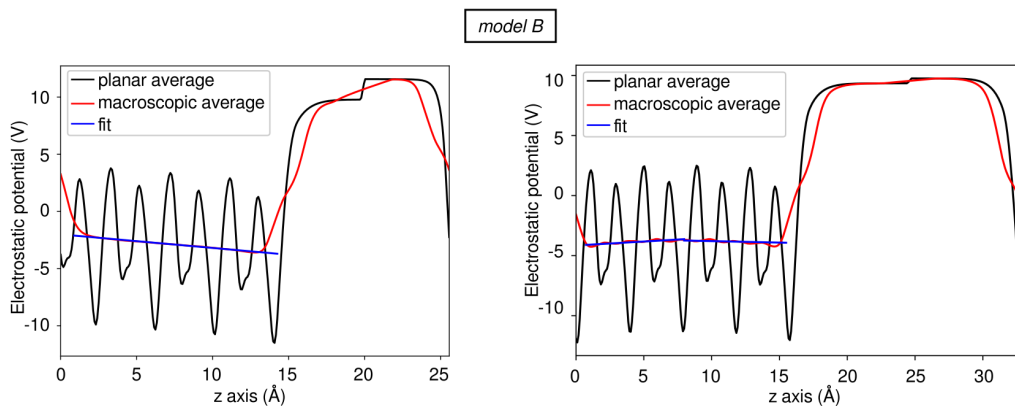


Fig. S1 Electrostatic potentials for the unrelaxed model B 0:4 La-terminated asymmetric (left) and symmetric (right) slab.

In Table S1, we show the surface and anion exchange energies for La and Ti terminations of surfaces constructed from both model A and B as a function of the number of exchanged layers. While for the La-terminated surface, there is a continuous increase of the surface energy, independent of the model, the surface energy for the Ti-termination drops below that of the purely *cis* surface (0:4) for up to two exchanged layers (2:4). An analysis of the anion exchange energy without relaxation (E_{ionex}^{urlx} , Eq. S1) shows that only the Ti-terminated surface of model B favourably exchanges one layer of anions, while relaxation effects (E_{ionex}) lead to the aforementioned preference for up to two exchanged layers for both models A and B.

$$E_{ionex}^{urlx} = E^{urlx}(x:4) - E^{rlx}(0:4), \text{ for } x=(1,3) \quad (\text{S1})$$

$$E_{ionex}^{rlx} = E^{rlx}(x:4) - E^{rlx}(0:4), \text{ for } x=(1,3) \quad (\text{S2})$$

We compute surface energies for asymmetric slabs using the approach developed by Eglitis.² In a first step, we determine the energy E_{cleave} required to break the bonds, so as to create two surfaces, as given in Eq. S3, where E_{slab}^{urlx} is the energy of the unrelaxed slab and E_{bulk} is the energy of bulk cell containing the same number of atoms. We assume that the energy to create the surface is evenly shared between the two terminations, which is the reason for the factor $\frac{1}{2}$. Next, we estimate the amount of energy gained as a result of the relaxation, E_{relax} in Eq. S4, as the difference in energy between the relaxed (E_{slab}^{rlx}) and unrelaxed (E_{slab}^{urlx}) slab. This energy is specific for each of the two surface termination. Since the bottom of the slab is kept fixed, it offers a way to differentiate between the two chemically distinct terminations. Finally, we determine the surface energy, E_{surf} in Eq. S5, as the sum of these two contributions per surface area.

$$E_{cleave} = \frac{1}{2}(E_{slab}^{urlx} - E_{bulk}) \quad (S3)$$

$$E_{relax} = E_{slab}^{rlx} - E_{slab}^{urlx} \quad (S4)$$

$$E_{surf} = \frac{E_{cleave} + E_{relax}}{A_{surf}} = \frac{2E_{slab}^{rlx} - E_{slab}^{urlx} - E_{bulk}}{2A_{surf}} \quad (S5)$$

We assume that the process of surface creation with anion reordering happens in two steps - first, the surface is cleaved from the bulk structure and then the anion exchange occurs, which is the reason why E^{urlx} is chosen to be that of models A or B with no anion exchange; subsequently, the surface relaxes into a slab with the chosen anion order. E_{bulk} is the bulk energy of each model and A_{surf} is the surface area.

Table S1 LaTiO₂N (001) surface energy (E_{surf}) and anion exchange energy (E_{ionex}) of both La and Ti terminations in the model slabs with different *trans*:total ratios constructed from models A and B (see Figure 2).

Termination	<i>trans</i> :total (layers)	E_{surf} (J/m ²)		E_{ionex} (eV)		E_{ionex}^{urlx} (eV)	
		model A	model B	model A	model B	model A	model B
La	0:4	1.161	1.255	-	-	-	-
	1:4	1.456	1.590	1.15	1.32	2.25	5.40
	2:4	1.612	1.776	1.75	2.06	4.53	8.87
	3:4	1.752	1.957	2.29	2.77	5.32	11.08
Ti	0:4	1.145	1.448	-	-	-	-
	1:4	0.930	0.997	-0.84	-1.78	0.09	-0.12
	2:4	1.024	1.159	-0.47	-1.14	1.99	2.89
	3:4	1.196	1.511	0.20	0.25	3.09	5.68

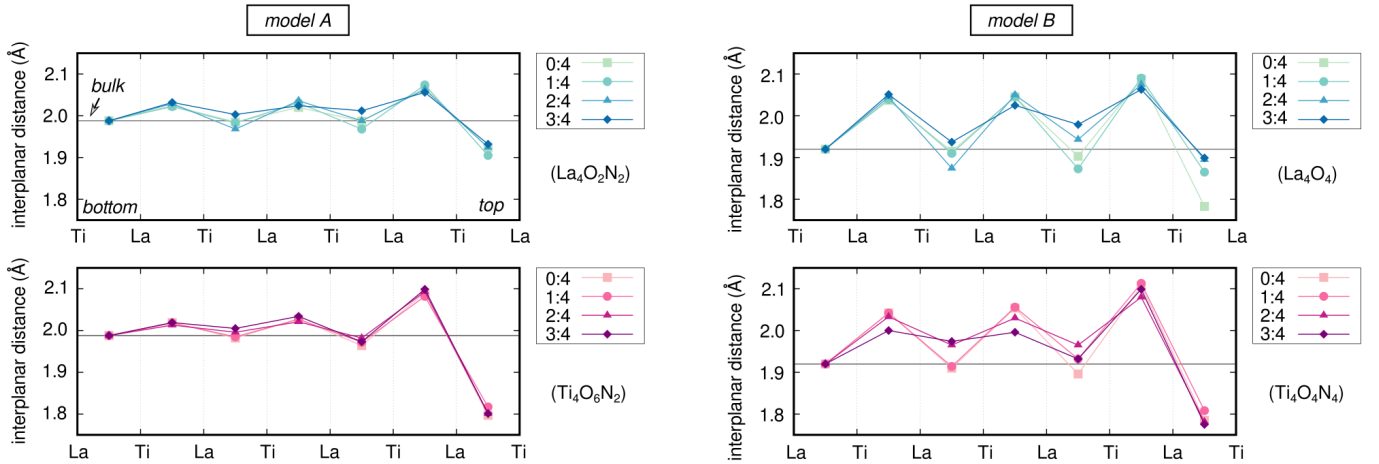


Fig. S2 Displacements in the models A (left) and B (right) of the $2 \times 2 \times 4$ simulation cell for the La (top panels) and Ti (bottom panels) terminations. The geometry optimization is carried out by relaxing all atoms, except for those in the bottommost unit cell, which are kept fixed at bulk positions.

In Figure S2, we report the change of the interplanar distance as a function of the *trans*:total ratio for both terminations and both models. As we can see, model A has generally smaller changes in the interplanar distances compared to model B. In general we observe an inward relaxation of the surface layer, followed by an oscillating inwards/outwards relaxation sequence. While the La termination of Model A shows a systematic change as a function of the *trans*:total ratio going towards a more uniformly expanded surface without oscillations, the Ti termination shows no large changes. Model B surfaces in general show larger changes as a function of the *trans*:total ratio also moving from oscillatory to more uniformly expanded with increasing number of *trans* layers. The interplanar spacings between the first and second as well as second and third layer are numerically given in Table S2, along with the rumpling of oxygen and nitrogen atoms in the surface layer. In general, we see that the anion exchange decreases the rumpling in the surface layer.

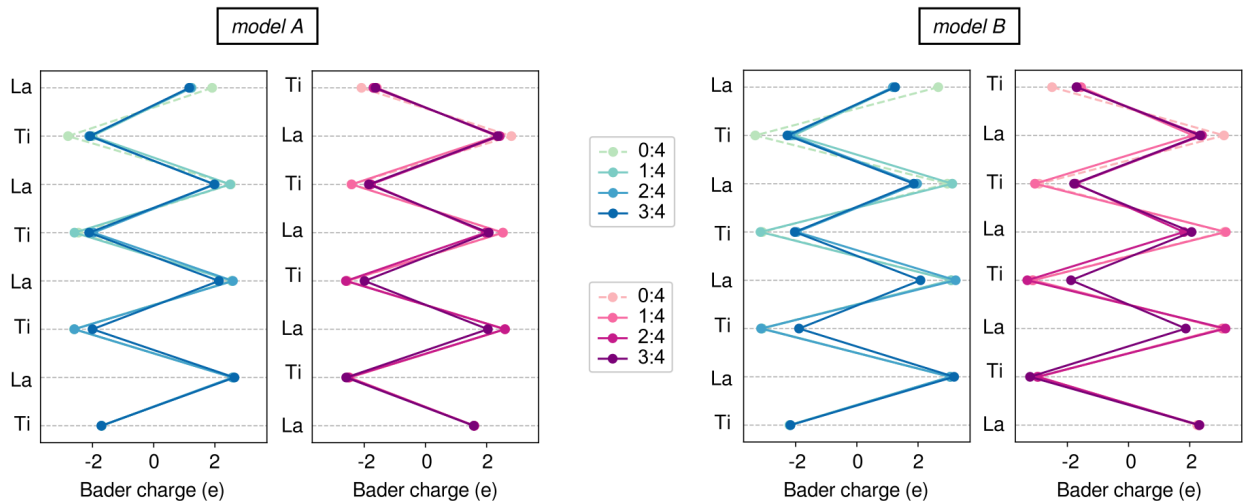
Table S2 Geometry characteristics of the surface layers in all slab models.

Model	Termination	<i>trans</i> :total	Δ_{1-2} (%) ^a	Δ_{2-3} (%) ^a	s_O (Å) ^b	s_N (Å) ^b
model A	La	0:4	-3.2	3.9	0.288	0.170
		1:4	-4.2	4.3	-	0.105/0.119
		2:4	-3.2	3.8	-	0.100
		3:4	-2.8	3.4	-	0.091/0.114
	Ti	0:4	-9.6	5.2	-0.258/-0.181/0.332	0.075
		1:4	-8.6	4.7	-0.158/-0.058/0.128/0.371	-
		2:4	-9.4	5.3	-0.103/0.009/0.072/0.314	-
		3:4	-9.4	5.6	-0.091/0.029/0.050/0.299	-
model B	La	0:4	-7.1	4.6	0.387	-
		1:4	-2.8	4.8	-	0.132
		2:4	-1.3	4.0	-	0.114
		3:4	-1.1	3.4	-	0.105
	Ti	0:4	-7.0	5.6	-0.338	0.208
		1:4	-5.8	5.9	-0.170/0.324	-
		2:4	-7.2	4.2	-0.146/0.306	-
		3:4	-7.5	5.2	-0.142/0.303	-

^a The interplanar distances, Δ , are calculated as the difference between the averaged topmost atomic layer heights with respect to the bulk value along that specific direction.

^b The rumpling, s , is calculated as the difference along z between the O or N atoms and the plane formed by the metal ones.

In Figure S3, we report the layer-averaged Bader charges^{3,4} for different thicknesses of anion-exchanged layers. As expected, the charge in the exchanged layers is lower than in the *cis* part for all models and terminations. Nonetheless, the resulting charge distribution is different from the one based on formal charges (see Figure 2). This is likely due to the reduced coordination number of the surface atoms and the resulting weak dipole is due to covalency effects.⁵ The exchanged atomic layers are, thus, polar-compensated and not non-polar lacking any charge accumulation/depletion.

**Fig. S3** Bader charges per layer with the anion exchange for the two models in the $2 \times 2 \times 4$ slab.

In Figure S4 we report the layer-resolved projected density of states for model A. The changes as a result of the different anion order at the topmost surface layer are similar to those observed in model B (see Figure 4 in the main text), however, pronounced to a lesser extent.

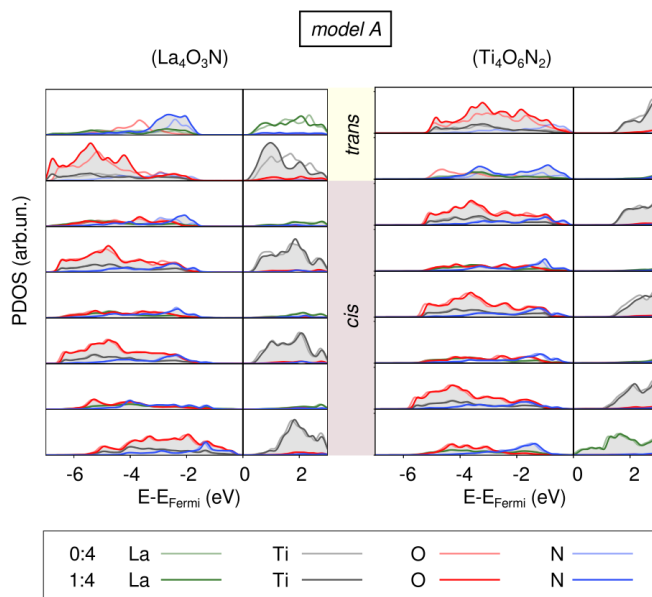


Fig. S4 Layer-resolved PDOS of both terminations in model A, where the 1:4 slab is drawn together with the 0:4 slab. The PDOS of model B are in the main text, Figure 4.

S1.1 Additional surface models

Here we present surface calculations obtained with slab models that have dimension $\sqrt{2}/2 \times \sqrt{2}/2$ -R45° with respect to the 2×2 supercell used in the above calculations. The reduced lateral dimensions allows us to consider thicker slab models to verify if our main conclusions are affected by artefacts resulting from our slab setup (4x model used in the main text). As shown for Model A La- and Ti-terminated surfaces in the left column of Figure S5, the relaxation of the surface layer is not affected by the limited thickness of our slab as we observe an upwards shift of the same relaxation pattern at the surface and the underlying layers with increasing slab thickness. As shown in the right column of S5, keeping the bottom layer frozen does also not affect the relaxation pattern at the surface.

In Table S3, we show the anion exchange energies without (E_{ionex}^{urlx}) and with (E_{ionex}) relaxation for both Model A and B as well as the La and Ti termination. We consider slabs that have the asymmetric geometry with a fixed bottom layer as in our standard setup (asymm), an asymmetric slab, where the fixing of the bottom layer is omitted (frlxasymm) and a symmetric slab setup with one additional atomic layer at the bottom of the slab (symm). We can see that while for model A there is a large difference between the symmetric and asymmetric slabs without relaxation, this difference is reduced to almost nothing when the models are relaxed. We can thus see that the different slab setups lead to very similar E_{ionex} for the different models and terminations, slight differences occurring for 3:4 ratios when the bottom of the slab is allowed to relax. More importantly though the slab setup does not affect our qualitative conclusions that only the Ti terminated surface has negative E_{ionex} for up to two layers.

Table S3 Exchange energies for the two models A: $\text{La}_4\text{O}_2\text{N}_2/\text{Ti}_4\text{O}_6\text{N}_2$ and B: $\text{La}_4\text{O}_4/\text{Ti}_4\text{O}_4\text{N}_4$. The E_{ionex}^{urlx} determines the energy difference between the relaxed 0:4 models and the unrelaxed mixed one, where just the anion exchange has occurred. E_{ionex} , on the other hand considers the relaxation as well.

		E_{ionex}^{urlx} (eV)			E_{ionex} (eV)				
		model A		model B	model A			model B	
Termination	<i>trans</i> :total (layers)	asymm	symm	asymm	asymm	frlxasymm	symm	asymm	frlxasymm
La	1:4	2.25	2.70	5.40	1.15	1.15	1.01	1.32	1.48
	2:4	4.53	4.51	8.87	1.75	1.76	1.57	2.06	2.30
	3:4	5.32	6.44	11.08	2.29	2.11	2.12	2.77	2.59
Ti	1:4	0.09	1.84	-0.12	-0.84	-0.83	-0.82	-1.78	-1.86
	2:4	1.99	3.48	2.89	-0.47	-0.52	-0.39	-1.14	-1.29
	3:4	3.09	5.38	5.68	0.20	0.12	0.24	0.25	-1.08

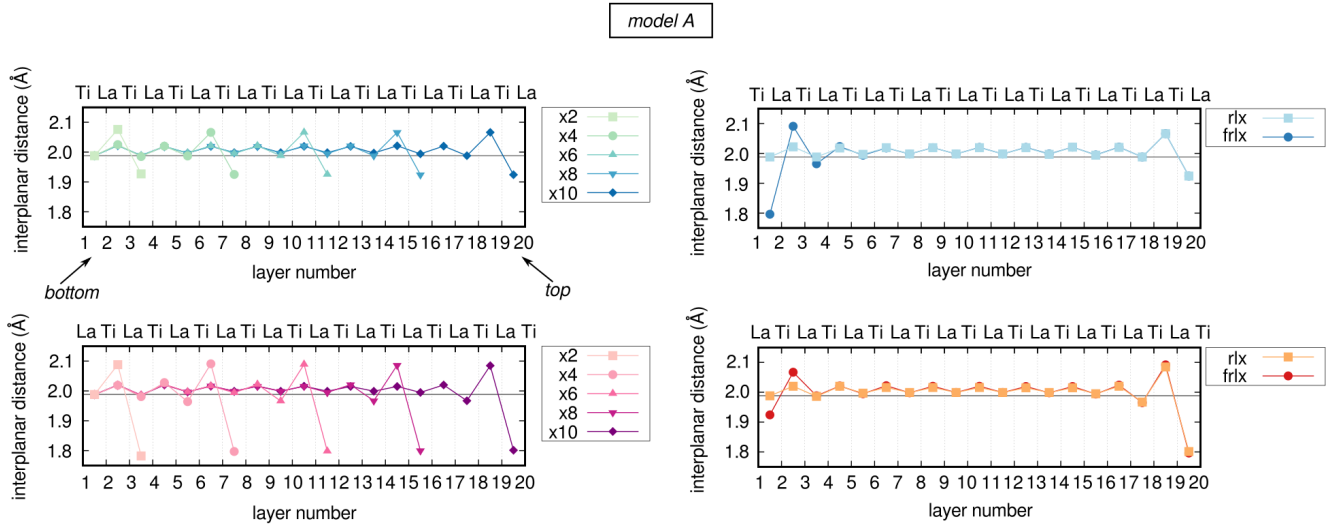


Fig. S5 Left column: interplanar spacings in the lateral $\sqrt{2}/2 \times \sqrt{2}/2$ -R45° simulation cell with n unit-cell layers thickness of the slab model. All atoms were relaxed, except for those in the bottommost unit cell, which were kept frozen at their bulk positions. Right column: comparison of interplanar spacings between a fully relaxed 10-layers slab (frlx, no frozen atoms) and one where the bottommost unit cell is kept fixed as in our standard setup (rlx). Top row: La-termination, bottom row: Ti-termination.

In order to evaluate if the proximity of the frozen bottom layer or the small thickness of the slab could have an effect on the observed E_{ionex} , we repeat the calculations for model A also with a thicker 6-layer slab. The results shown in Table S4, show that the results are qualitatively and even quantitatively the same, only the Ti termination having negative E_{ionex} for up to two *trans* layers at the surface. We thus conclude that the slab setup used in the main text has no effect on our conclusions as the same results are obtained with thicker or differently constructed slabs.

Table S4 Surface and anion exchange energies of the 6-layered model A slab with different *trans*:total ratios. The same lattice parameters are used as for the 4-layered slab.

Termination	Mixing ratio Mixing ratio	model A	
		E_{surf} (J/m ²) ^a	E_{ionex} (eV)
La	0:6	1.115	-
	1:6	1.408	1.14
	2:6	1.570	1.77
	3:6	1.708	2.31
	4:6	1.847	2.84
	5:6	1.974	3.34
Ti	0:6	1.104	-
	1:6	0.891	-0.82
	2:6	0.983	-0.47
	3:6	1.123	0.07
	4:6	1.267	0.64
	5:6	1.436	1.29

S2 Polar interface

In Figure S6 we show the layer-resolved projected density of states of the polar interfaces constructed from model A bulk. The polarity in this model is weaker and it fails to reach band-inversion and electron/hole doping of the interface for the overlayer thicknesses investigated here.

In Figure S7, we show the plane-averaged and macroscopic electrostatic potential for the n- and p-type interfaces constructed from bulk model B. For the n-type interface we see an internal electric field in both the *cis* and *trans* part that increases with increasing *cis* layer thickness. For the p-type interface, there is no field in the *trans* part and only the *cis* part shows a field that is weaker than in the n-type interface.

In figure S8a, we show the Bader charges in each layer of the two types of interfaces with different *trans* overlayer thicknesses. For the n-type interface there is a gradual change in charge for planes in the *trans* layer and close to the interface. This charge is

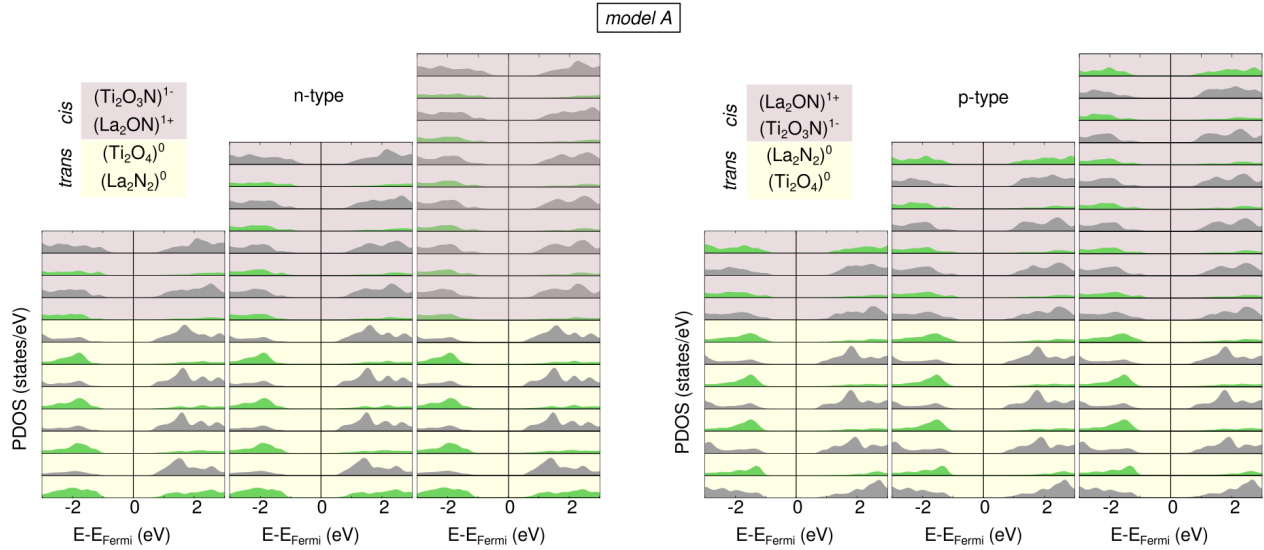


Fig. S6 Layer-resolved total PDOS of the polar interface for model A, for different thicknesses of the *cis*-ordered layer. In green we indicate the La-atomic layers and in grey - the Ti ones. The p-type interface is on the left and the n-type on the right. The corresponding data for Model B is presented in the main text, Figure 6.

transferred from the surface Ti layer, where the absolute value of the Bader charge decreases. No such charge transfer is observed for the p-type interface, where both the charges close to the interface as well as the La surface layer remain constant. We thus correlate the amount of transferred charge with the dipole as a measure proportional to the internal field only for the n-type interface. As shown in figure S8b, the amount of transferred charge correlated with the dipole but shows a decreasing trend for thicker *cis* overlayers and thus polarisations, which can be seen as a measure for the polarity compensation.

In Figure S9, we analyze the geometry of the model B interfaces in terms of interlayer spacings, octahedral tilts and Ti-X bond lengths along the interface normal direction. In terms of inter-layer spacings, both the n- and p-type interface show strong oscillations in the polar *cis* part of the slab for thin overlayers. Interestingly though, these oscillations completely disappear once the slab becomes solidly metallic for the 4:6 n-type interface. We see in general strongly suppressed octahedral rotations in the *trans* part of the interface compared to the corresponding bulk value. For the n-type interface the bulk tilt angle is only recovered for the metallic 4:6 slab, whereas for the p-type interface a bulk-like structure is already recovered for the 4:4 slab. Besides changes in octahedral rotation magnitudes, we also observe a favoring of in-phase octahedral rotations around the interface normal direction in the *trans* part of the slab, which is complete for the n-type and partial for the p-type interface.

Similarly to other oxide interfaces, the strong suppression of octahedral tilts in the non-polar part of the interface can lead to the appearance of polar distortions to optimise bonding in the perovskite structure.⁶ We see these polar distortions emerging as strong oscillations of the Ti-X bond lengths, where up- and down-oriented bonds of the same Ti differ by about 0.24Å. Such polarity was also seen in the *trans*-ordered bulk.⁷ For all p-type interfaces as well as the 4:2 n-type interface we observe opposite displacements of Ti-X bonds for different Ti in the same layer. This implies an anti-ferroelectric type distortion, which will however have a similar effect on orbital energies as a purely ferroelectric one observed in n-type 4:4 and 4:6.

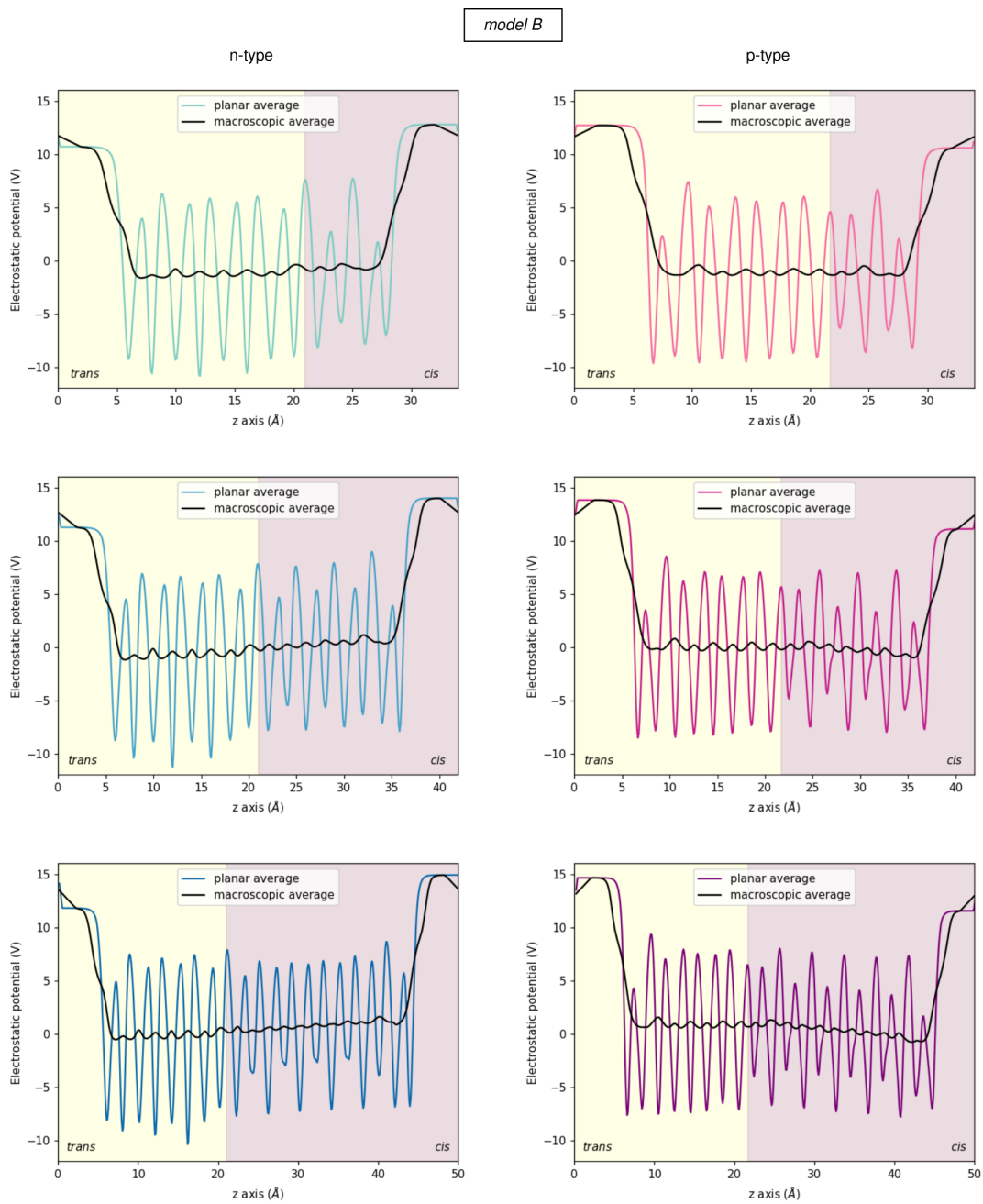


Fig. S7 Plane-averaged and macroscopic electrostatic potentials for the polar/non-polar interfaces with different polar overlayer thicknesses constructed from bulk model B.

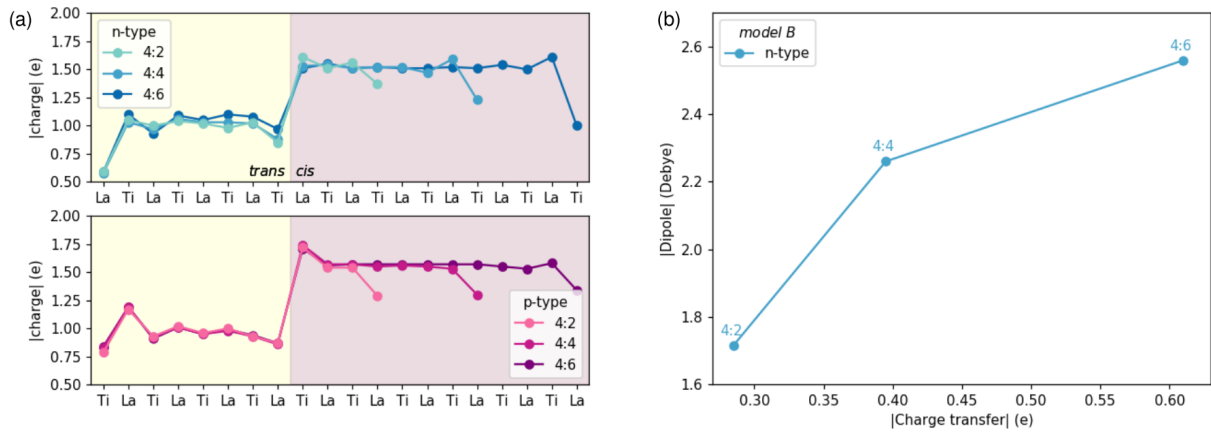


Fig. S8 a) Absolute values of Bader charges per layer for the two interface types and different *cis*-layer thickness. b) Correlation between the dipole moment and the charge transferred from the *cis*- to the *trans*-ordered interface part, both quantities are shown as absolute values.

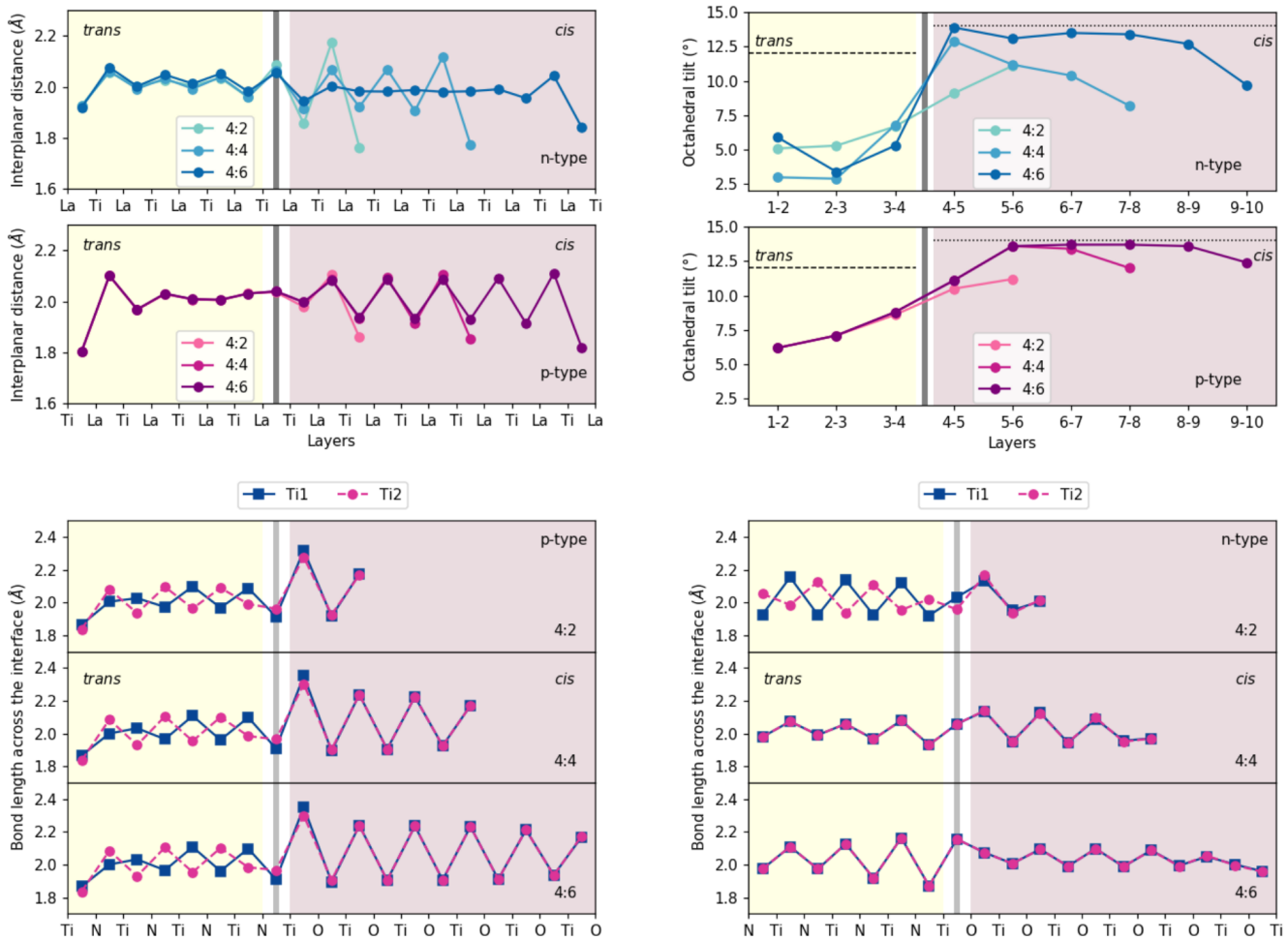


Fig. S9 Interplanar distances, octahedral tilts and Ti-X (X=O,N) bond lengths along the normal of the interface in Model B p-type and n-type interfaces. Ti1 and Ti2 correspond to each of the two Titanium atoms within each layer of the polar-interface models.

References

- 1 C. Cheng, K. Kunc and M. H. Lee, *Phys. Rev. B*, 2000, **62**, 10409–10418.
- 2 R. I. Eglitis and D. Vanderbilt, *Phys. Rev. B*, 2007, **76**, 155439.
- 3 R. F. Bader, *Atoms in Molecules*, Clarendon Press, Oxford, 1990, vol. XVIII.
- 4 W. Tang, E. Sanville and G. Henkelman, *Journal of Physics: Condensed Matter*, 2009, **21**, 084204.
- 5 C. Noguera, *Journal of Physics: Condensed Matter*, 2000, **12**, R367.
- 6 J. Gazquez, M. Stengel, R. Mishra, M. Scigaj, M. Varela, M. Roldan, J. Fontcuberta, F. Sánchez and G. Herranz, *Physical Review Letters*, 2017, **119**, 106102.
- 7 N. Vonrüti and U. Aschauer, *Physical Review Materials*, 2018, **2**, 105401.